

Author: Bryan Crawford, *Director of Analytical Services*

Samples

Six low-k thin film samples were chosen to conduct scratch tests to further evaluate the mechanical integrity of the films. Elastic modulus and hardness testing had already been completed on the samples. These six samples were chosen from a boat of samples because they formed two groups – consisting of three wafers in each group – in which the elastic moduli and hardness of the samples were statistically identical. All of the wafers were composed of nominally the same materials but were subjected to slight changes in processing. Scratch testing is used to further evaluate how processing might have affected the interface strength of the samples. The film thicknesses ranged from 569 nm to 622 nm – which is within a 10% range in film thickness; this is the thickness range that Nanomechanics, Inc. has determined ideal for the comparison of scratch results. If the film thicknesses are scattered about a range that is larger than 10%, film thickness will start having a larger influence in the results of film failure. Figure 1 shows the six samples mounted and ready for testing.

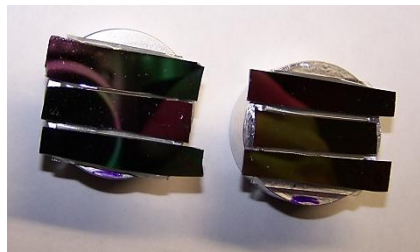


Figure 1: Six diced wafer samples mounted on 1.25" sample pucks and ready for testing.

Test Protocol

A progressive load scratch test was used to conduct 5 tests on each sample. The scratch tests completed at Nanomechanics, Inc. consists of three steps: 1. the scratch tip is used to perform a single-line profile of the scratch path; 2. the tip returns to the origin and the progressive load scratch test is performed along the same path; 3. the tip returns to the origin again and the completes a residual deformation scan of the scratch path. A short distance is scanned prior to and after each of the three test segments. This scan is usually equal to about 10% of the scratch distance and is used for aligning the displacement data collected for the three segments. During the second step when progressive loading is taking place, the instrument continuously examines the data and looks for film failure. If film failure is detected, the system automatically stops the loading segment to prevent tip damage from it being dragged through substrate materials. The scratch process is diagramed in Figure 2 and the results from a scratch test (in the form of scratch curves) are shown in Figure 3.

Figure 3 shows the scratch curves all aligned on one graph so that the scratch deformation can be correctly interpreted. In the scratch curves, 2 distinct modes of failure are identified with the critical load markers LC1 and LC2; the failure types are discussed in the Results section. Displaying all of the steps on one graph has the distinct advantage that it makes it easy to quantify the dominate deformation mechanisms leading up to failure. Figure 4 shows the same curves that are displayed in Figure 3 but it identifies the areas of elastic deformation (hashed out in red) and plastic deformation (cross-hatched in grey) leading up to the initial point of failure; this particular sample exhibited a large amount of elastic deformation during the initial portion of the scratch test. These areas are used to quantify the percent of elastic and plastic deformation in the results.

The tip chosen for conducting the scratch tests was a cube corner tip with a tip radius that had an effective tip radius of approximately 340 nm. This tip geometry is a three-sided pyramid and it creates high levels of stress in the material during the scratch test. Scratches can be performed either face-forward or edge-forward when using a pyramid shaped indenter. Scratching face-forward with the cube-corner tip acts like a snow plow and creates very high lateral stresses in the film, while edge-forward cuts the material like a knife. A diagram of a cube corner tip is shown in Figure 5. The low-k samples were tested using the cube-corner tip positioned so that it scratched face-forward.

When performing scratch testing on any sample set, it is critical that all test parameters and tip geometries remain consistent throughout the samples being compared. The test parameters used in testing the low-k materials are listed in Table 1.

Table 1: Parameters used in the progressive load scratch tests

Scratch Length	100 μ m
Scratch Velocity	20 μ m/s
Maximum Scratch Load	1mN
Tip Geometry	Cube-Corner (Effective tip radius: 340 nm)
Scratch Direction	Face Forward

ServiceLab@nanomechanicsinc.com

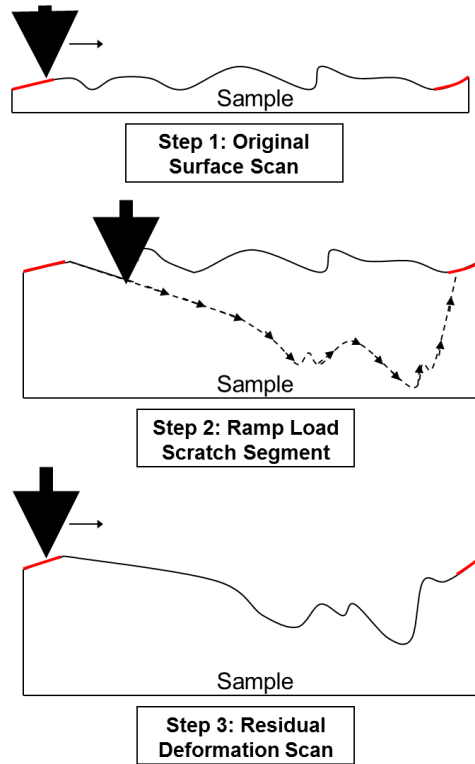


Figure 2: Diagram of the three-step progressive-load scratch test. Red lines show the areas of pre and post profile scans used to perform leveling of the 3 steps and to match the curves on one graph.

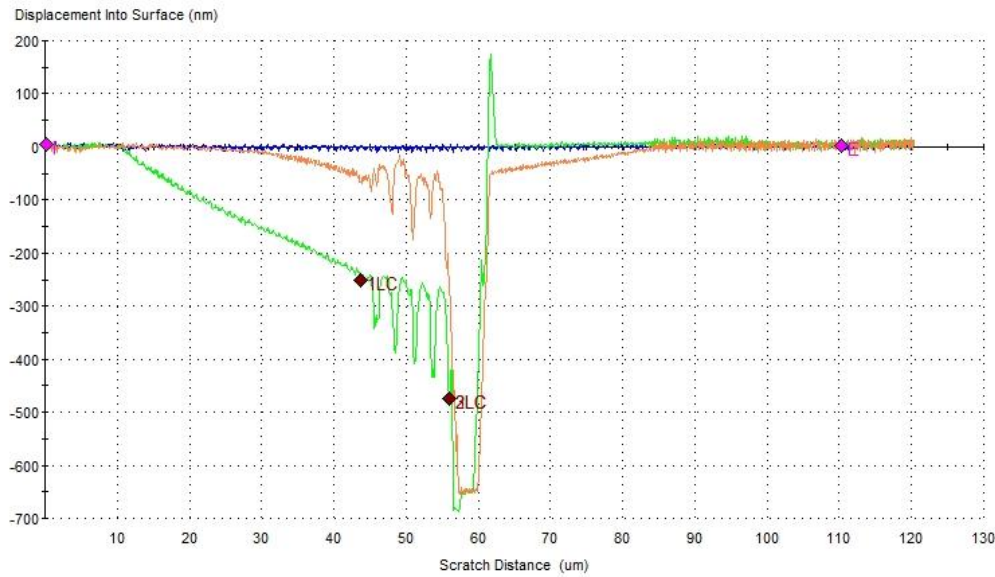


Figure 3: Typical displacement curves from a scratch test on a low-k film; the blue trace along the x-axis is the single-line original topography scan (Step 1), the green curve is the scratch cycle (Step 2), and the orange curve is the residual deformation scan (Step 3) – all displayed on one graph.

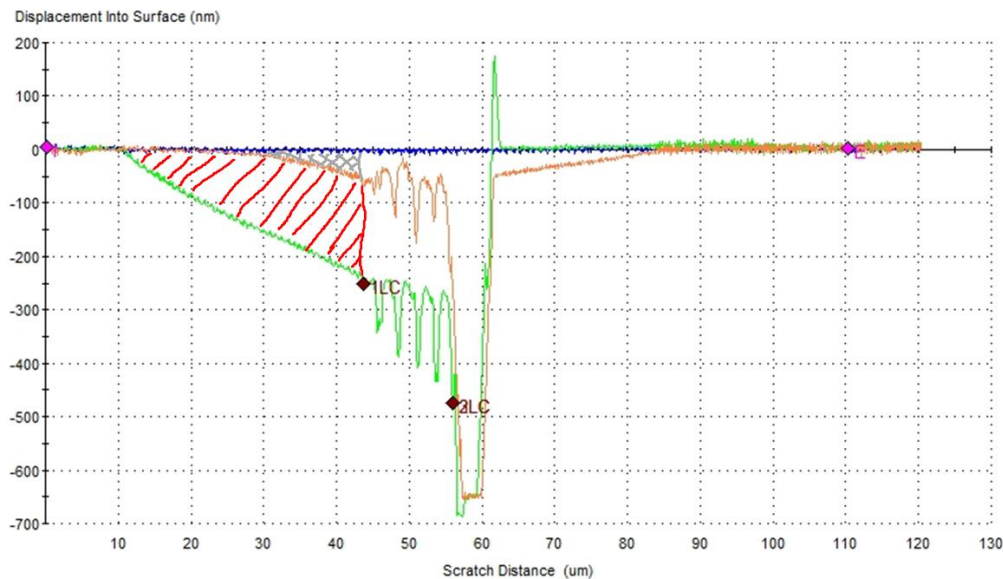


Figure 4: Same scratch curves as displayed in Figure 3, but the elastic deformation - the region between the scratch cycle and the residual deformation scan - is hashed out in red and the plastic deformation – the region between the original topography scan and the residual deformation scan - is cross-hatched in grey.

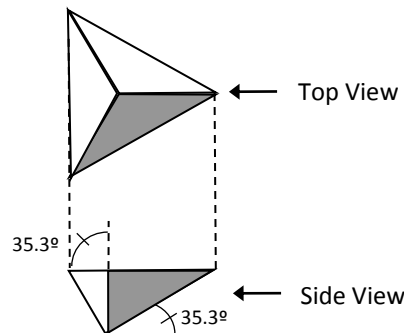


Figure 5: Diagram of a cube-corner tip.

Results

All of the samples were first tested using nanoindentation to determine the elastic modulus and hardness of the low-k film samples; these results are displayed in figures 6 and 7, respectively. The results for elastic modulus were analyzed using the Hay-Crawford analysis which provides substrate independent results for thin films [1]. A summary of the results for the elastic modulus and hardness of the films are provided in Table 2; this table lists both the results for the elastic modulus (substrate corrected results using the Hay-Crawford model) and hardness at 10% of the penetration in addition to the minimum properties of elastic modulus and hardness using the standard Oliver-Pharr analysis with the continuous stiffness measurement technique [2]. For convenience, a description of each result is provided below the summary in Table 2.

Scratch testing was completed to further evaluate how processing might have affected the mechanical integrity of the low-k samples. As opposed to standard indentation testing which imposes semi-static stresses that propagate throughout the film and sample, scratch testing imposes large dynamic lateral stresses at the surface of the sample and, as the test progresses, this stress gradually builds up at the interface between the film and substrate. Typically, during a scratch test, lateral fracturing or buckling of the film occurs first, and, then, is followed by recovery spallation of the film where the lateral fractures propagate through the film but they sufficiently alleviate stress levels to keep the film from total separation. Finally, as the normal forces and, consequently, the lateral forces increase, the film experiences gross spallation (complete delamination). Failure during a scratch test can evolve in a unique manner depending on the sample. For example, some films may experience blistering (interface separation) as opposed to lateral fracturing or recovery spallation – in this instance, the residual deformation scan clearly shows the blistering effect in the displacement curves. A summary of the scratch results and failure types for the six low-k samples are provided in Table 3 - descriptions of the results are provided below the table.



Analytical Services Laboratory
105 Meco Lane
Suite 100
Oak Ridge, TN 37830
(865) 978-6490 Ext. 300

ServiceLab@nanomechanicsinc.com

Typically, scratch tests on low-k samples are highly repeatable. Figure 8 shows the scratch curves for all of the tests completed on wafers 1 and 12 – all of the samples had repeatability as good as the samples displayed in this figure. Deformation and failure mechanisms are shown to be highly repeatable with this scratch process.

Representative scratch curves from each of the samples are displayed in figures 9 through 14. The figures contain detailed descriptions of the failure modes that occurred due to the scratch tests. The figures also contain images of the scratches so that “fingerprints” of the failure mode can be recognized and used to evaluate other samples with similar failure modes. This system of fingerprinting failure helps to increase throughput - by not having to perform imaging of the resulting failures - of samples allowing larger numbers of tests to be conducted for higher statistical accuracy.

Figure 15 displays a bar graph of the initial failure for each of the samples (LC1); the error bars on each column cover one standard deviation in the results. Wafer 2 is seen as the sample that is most resistant to fracture and spallation; the results for this wafer, listed in Table 3, show that the *Percent of Plastic Deformation* is higher than most of the other samples, suggesting that this sample accommodates scratch deformation through plasticity as opposed to fracturing.

Wafer 2 is also shown to be the film with the highest resistance to gross spallation; a bar graph of the LC3 critical loads (gross spallation) is provided in Figure 16. Interestingly, LC1 failures (initial failures) in wafers 1, 2, and 12 tracked well with the ordering of performance in LC3 failures (gross spallation); however, the LC1 failures in wafers 3, 10, and 13 did not track well with the ordering of LC3 failures. It is important to identify which modes of failure are most critical to avoid during application and evaluate the results accordingly.



Analytical Services Laboratory
 105 Meco Lane
 Suite 100
 Oak Ridge, TN 37830
 (865) 978-6490 Ext. 300

ServiceLab@nanomechanicsinc.com

Table 2: Summary of the elastic modulus and hardness results for the low-k samples.

Sample	Elastic Modulus _ Film (9.5 % to 10.5 %)	Hardness (9.5 % to 10.5 %)	Minimum Apparent Modulus	Minimum Hardness	Depth At Min E	Depth At Min H	Drift Correction
	GPa	GPa	GPa	GPa	Angstroms	Angstroms	nm/s
W1	4.6	0.74	5.01	0.66	261	347	-0.028
W2	4.4	0.75	4.84	0.7	274	366	-0.074
W3	4.08	0.69	4.54	0.63	318	408	-0.098
W10	4.1	0.64	4.69	0.61	334	825	-0.05
W12	4.5	0.79	5.14	0.73	330	343	-0.027
W13	4.15	0.72	4.69	0.65	331	676	-0.038

Result Descriptions

Elastic Modulus _ Film (9.5 % to 10.5 %): Average elastic modulus of the film taken at penetrations depths between 9.5% and 10.5% of the film thickness. This result uses the Hay-Crawford model for providing substrate independent measurements of Young's modulus [1].

Hardness (9.5 % to 10.5 %): Hardness of the film taken at penetrations depths between 9.5% and 10.5% of the film thickness. This result is determined using the Oliver-Pharr technique and does not use analysis that accounts for substrate influences - the hardness of a film is rarely affected by the substrate at 10% of the thickness [2].

Minimum Apparent Modulus: The minimum elastic modulus measured during the indentation test at penetration depths greater than 20nm. This result is determined using the Oliver-Pharr analysis and does not use analysis that accounts for substrate influences. The elastic modulus of a film is often affected by the substrate or a skin-effect when indentation is performed on low-k films; by taking the minimum this is the best possible measurement of elastic modulus without using a model that takes substrate influences into account. This result is provided so that comparisons to historical data can be made.

Minimum Hardness: The minimum hardness measured during the indentation test at penetration depths greater than 20nm. This result is determined using the Oliver-Pharr analysis and does not use analysis that accounts for substrate influences - the hardness of a film is rarely affected by the substrate at, or under, 10% of the thickness.

Depth At Min E: Penetration depth at which the minimum measurement of elastic modulus was detected.

Depth At Min H: Penetration depth at which the minimum measurement of hardness was detected.

Drift Correction: Thermal drift of the sample as measured at the end of each indentation test; this value should always be below 0.1 nm/s.



Analytical Services Laboratory
 105 Meco Lane
 Suite 100
 Oak Ridge, TN 37830
 (865) 978-6490 Ext. 300

ServiceLab@nanomechanicsinc.com

Table 3: Summary of the scratch results and failure types for the 6 low-k samples.

Sample/Film thickness		LC1 Force	LC2 Force	LC3 Force	Failure Types	Percent Elastic Deformation	Percent Plastic Deformation
		mN	mN	mN		%	%
Wafer 1 622 nm	Mean	0.376		0.562	LC1 - Recovery Spallation	86.1	13.9
	Std. Dev.	0.012		0.044		1.8	1.8
	% COV	3.26		7.76	LC3 - Gross Spallation	2.06	12.79
Wafer 2 617 nm	Mean	0.542	0.698	0.83	LC1 - Buckling/Blistering	74.5	25.5
	Std. Dev.	0.006	0.025	0.019	LC2 - Recovery Spallation	2.1	2.1
	% COV	1.13	3.65	2.33	LC3 - Gross Spallation	2.83	8.26
Wafer 12 569 nm	Mean	0.409	0.573	0.7	LC1 - Buckling/Blistering	79.9	20.1
	Std. Dev.	0.01	0.055	0.01	LC2 - Recovery Spallation	1.6	1.6
	% COV	2.38	9.64	1.5	LC3 - Gross Spallation	1.96	7.77
Wafer 3 608 nm	Mean	0.346		0.448	LC1 - Spallation Recovery	87.1	12.9
	Std. Dev.	0.007		0.016		3.8	3.8
	% COV	2.03		3.55	LC3 - Gross Spallation	4.38	29.61
Wafer 10 599 nm	Mean	0.308	0.386	0.646	LC1 - Forward Cracking	73.5	26.5
	Std. Dev.	0.019	0.016	0.019	LC2 - Recovery Spallation	4.5	4.5
	% COV	6.13	4.13	2.87	LC3 - Gross Spallation	6.12	16.94
Wafer 13 600 nm	Mean	0.327		0.627	LC1 - Spallation Recovery	80	20
	Std. Dev.	0.014		0.007		3.8	3.8
	% COV	4.27		1.16	LC3 - Gross Spallation	4.8	19.23
Result Descriptions							
LC1 through LC3 - These results are the normal forces which caused distinct failure types in the samples. Typically, more than one failure type occurs during a scratch test.							
Failure Types - Type of failure that occurred at the critical load (LC forces) determined from the "fingerprints of failure" in the displacement curves generated by the scratch test. These samples have had imaging of the failure regions to ensure proper identification of failure.							
Percent Elastic Deformation - This is a measure of the elastic deformation leading up to failure in the film. Prior to LC1 (initial failure in the film), elastic and plastic deformations occur. The percent of elastic deformation is calculated by measuring the area between the line-profile generated by the scratch curve and the line-profile generated by the residual deformation scan up to the point of initial failure. This area is normalized by the total deformed area up to the point of initial failure.							
Percent Plastic Deformation - This is a measure of the plastic deformation leading up to failure in the film. The percent of plastic deformation is calculated by measuring the area between the line-profile generated by the original topography scan and the line-profile generated by the residual deformation scan up to the point of initial failure. This area is normalized by the total deformed area up to the point of initial failure.							

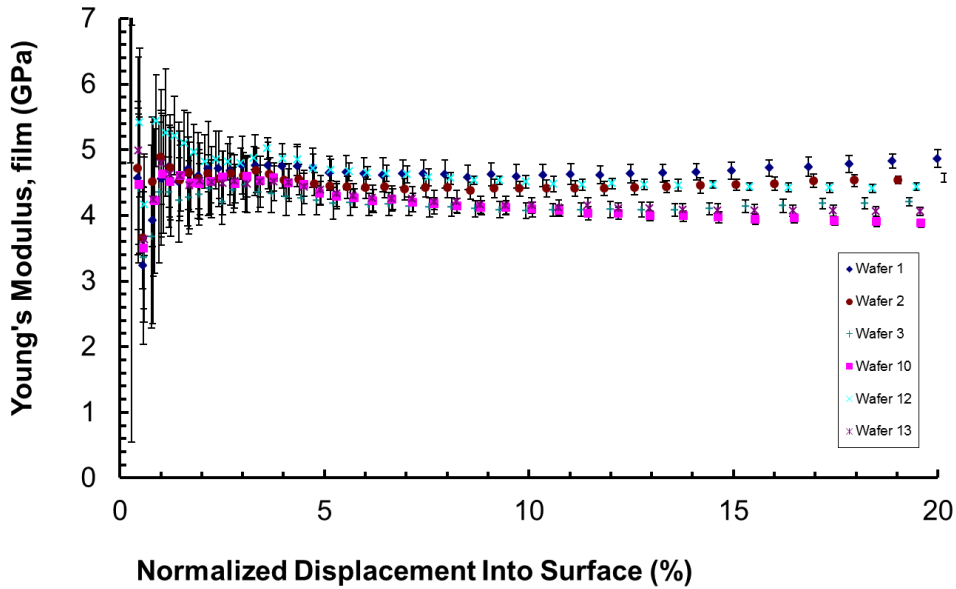


Figure 6: Elastic modulus of the six thin film samples versus normalized penetration into the film; notice that the data form two groups at 10% penetration with wafers 1, 2, and 12 forming the first group and wafers 3, 10, and 13 forming the second group.

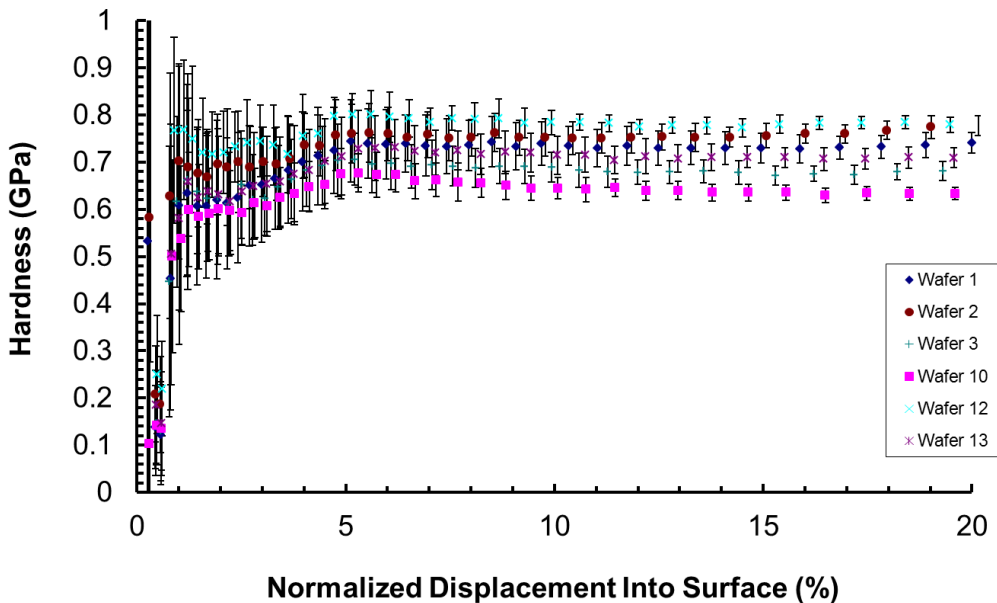


Figure 7: Hardness of the six samples as a function of normalized penetration depth; the two groups that are apparent in Figure 3 are not as apparent in the hardness data, but the samples still loosely group into the sets identified in Figure 6.

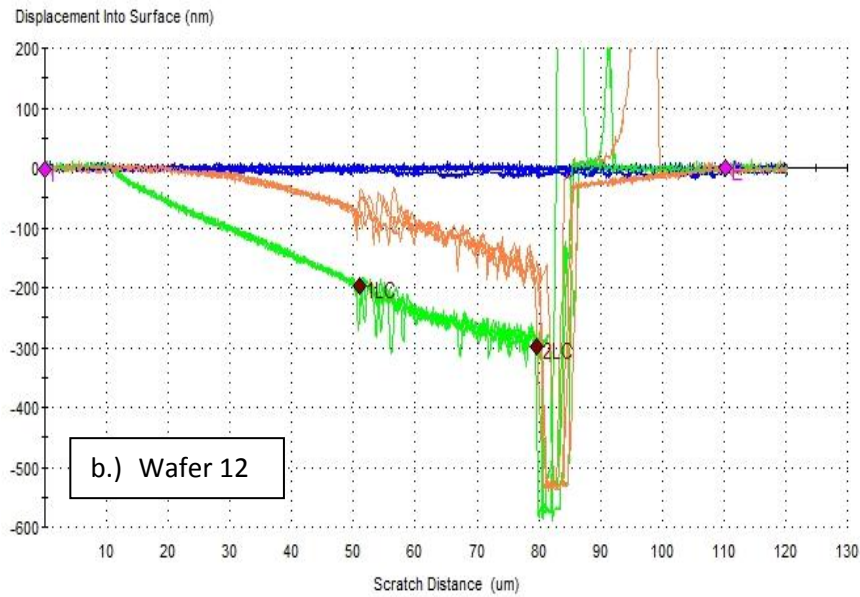
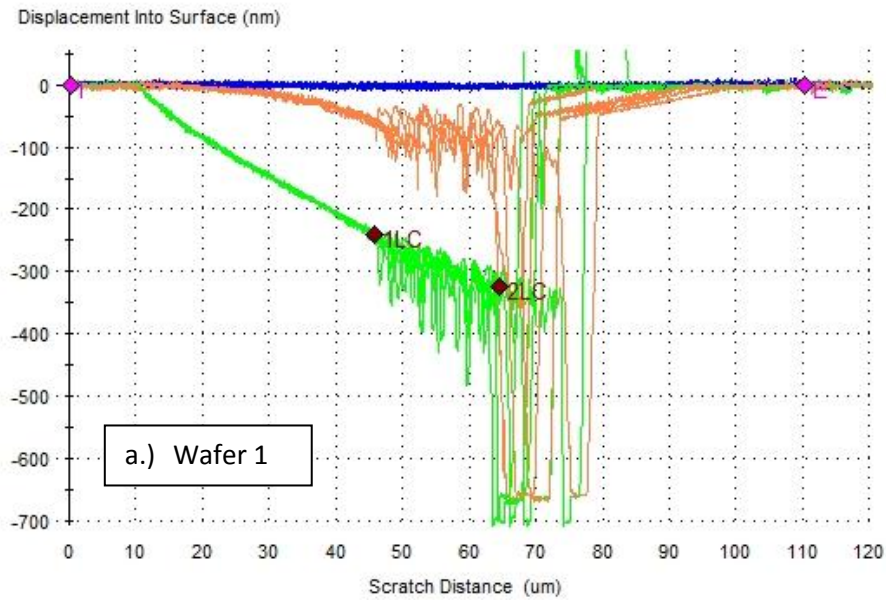


Figure 8: All of the tests on wafers 1 (graph a.) and 12 (graph b.) showing the repeatability of the deformation during the scratch tests and the repeatability of the results; the blue traces along the x-axis are the original topography scans, the green curves are the scratch cycles, and the orange curves are the residual deformation scans. Typically, all of the scratch tests on low-k film samples have this level of repeatability.

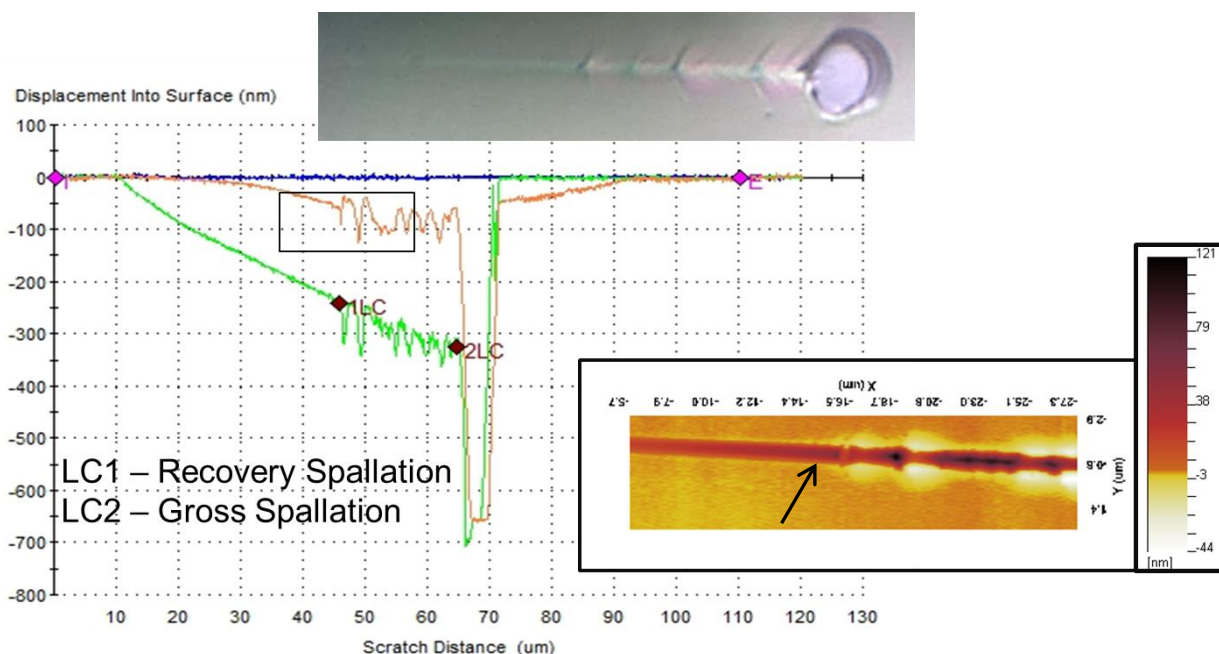


Figure 9: The figure shows typical displacement curves from the scratch tests on Wafer 1; the blue trace along the x-axis is the single-line original topography scan, the green curve is the scratch cycle, and the orange curve is the residual deformation scan. Recovery spallation and gross spallation are seen in the microscope image (taken at 3750X magnification) but they are also easily identifiable in the single-line residual deformation scan on the scratch curves at points 1LC and 2LC, respectively. The area within the black box identifies the initial recovery spallation zone and scanning probe microscopy was used to image this area and the resulting image is provided on the right side of the figure. Two points of failure are clearly shown: first, the large displacement oscillations in the 2-D graph showing displacement curves are seen as buckled areas with small rips on the side; secondly, just prior to the recovery spallation (in the area of the 3-D graph identified by the black arrow) rippling is seen in the film suggesting a minor amount of buckling may have occurred prior to, or as a result of, the failure identified by LC1.

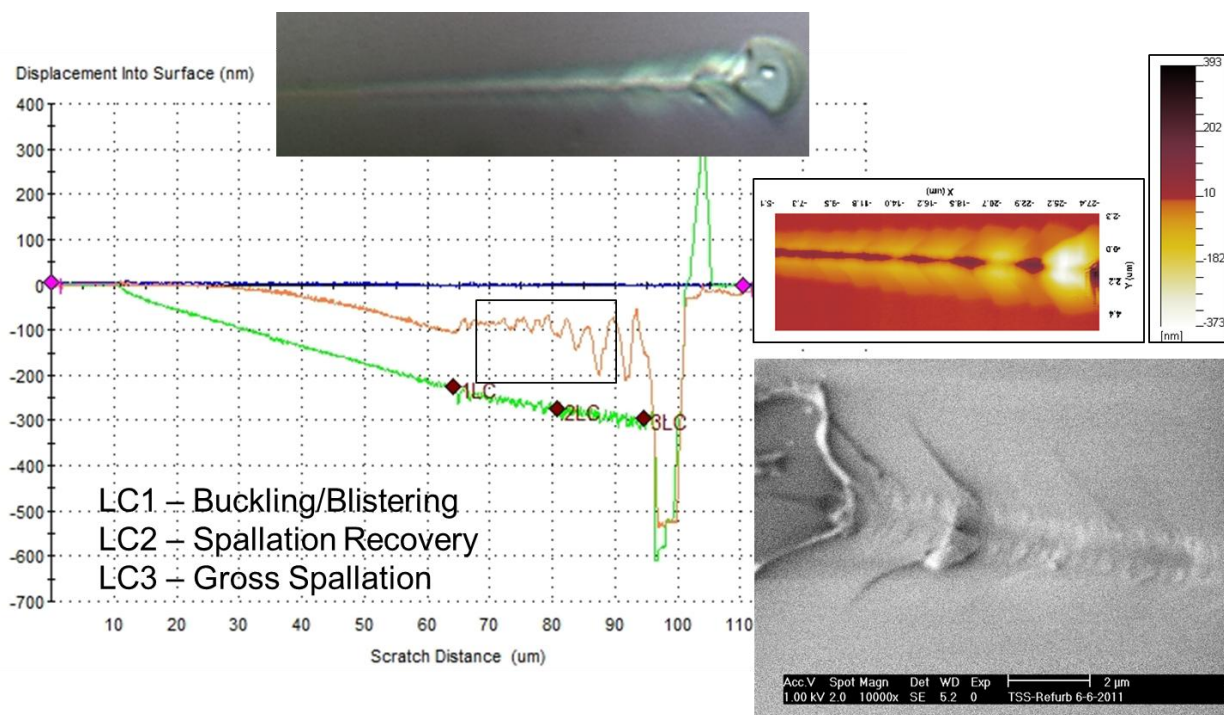


Figure 10: This figure shows typical displacement curves from the scratch tests on Wafer 2; the **blue** trace along the x-axis is the single-line original topography scan, the **green** curve is the scratch cycle, and the **orange** curve is the residual deformation scan. The failure mode at LC1 is distinctly different from that which occurred in Figure 9. Here an elevated region is observed which is due to the film lifting off of the substrate. The SEM image in the lower right shows the failure of one of the scratches performed on Wafer 2. This image shows a rippled trace leading up to the area of recovery spallation and lateral fracturing in the film. This rippled area is buckling of the film which is leading to larger scale blistering shown in the area identified by the black box on the scratch curves. The area in this black box was imaged using scanning probe microscopy and is shown to the right of the scratch curves. Recovery spallation is visible just at the end (right side) of the scanned region. The film in this region has blistered up from the substrate by about 200 nm propagating out from the scratch path by about 2 microns in each direction. The microscope image (taken at 3750X magnification) confirms the spallation recovery and gross spallation.

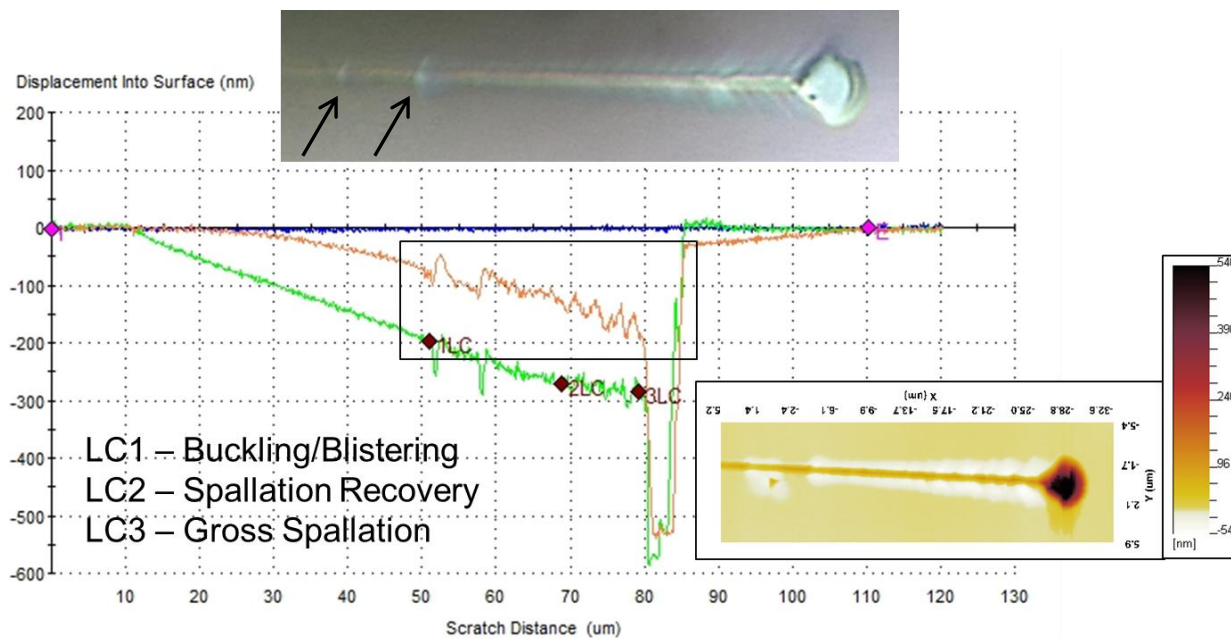


Figure 11: This figure shows typical displacement curves from the scratch tests on Wafer 12; the blue trace along the x-axis is the single-line original topography scan, the green curve is the scratch cycle, and the orange curve is the residual deformation scan. Mixed failure occurs for this sample at LC1; the initial failure is actually spallation recovery but this failure mode is not sustained for this sample until LC2 is reached. At LC1 spallation recovery starts the failure but then quickly switches to buckling of the film and blistering from the substrate. The microscope image above the scratch curves shows the initial failure in the areas identified by black arrows, but this failure is unsustainable. The scratch curves are key to identifying this failure, if spallation recovery continued there would be large displacement oscillations in the curves (similar to that of Figure 9); however, only small perturbations are seen after initial failure and the residual deformation scan shows a distinct step in the film height indicating blistering of the film. The area within the black box on the scratch curves was scanned using scanning probe microscopy and the image of this failure area is shown to the right of the figure. The initial failure is seen as the island along the scratch path prior to sustained blistering and finally film failure.

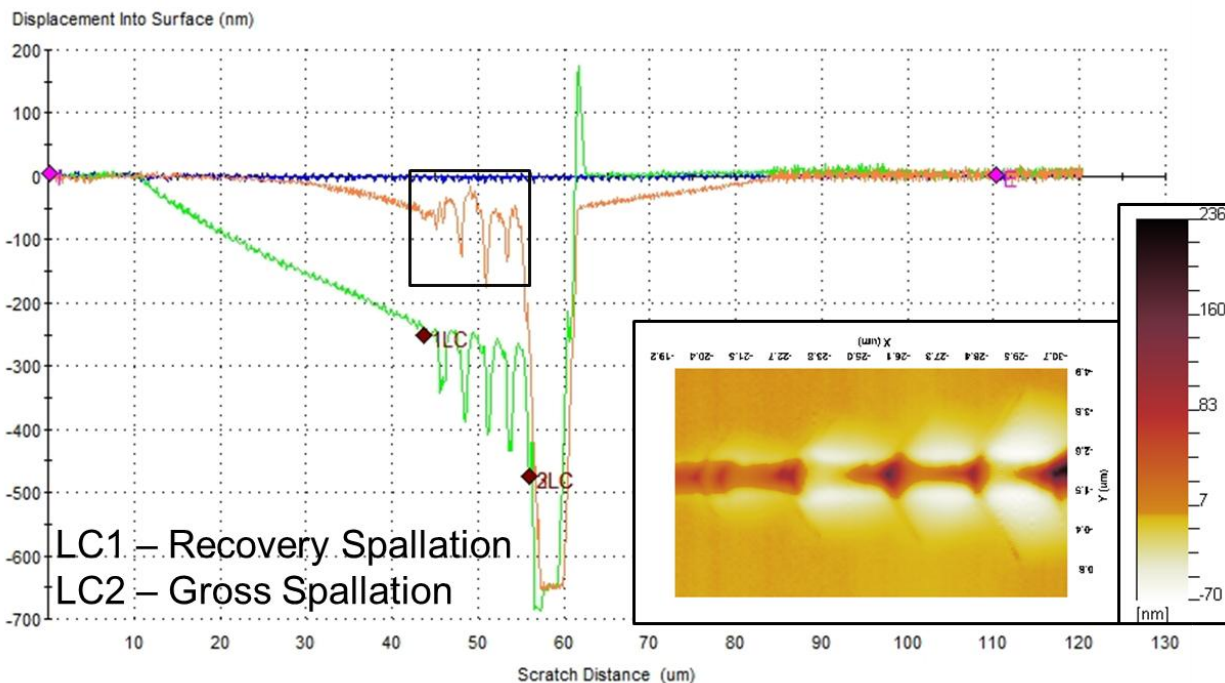


Figure 12: The figure shows typical displacement curves from the scratch tests on Wafer 3; the blue trace along the x-axis is the single-line original topography scan, the green curve is the scratch cycle, and the orange curve is the residual deformation scan. The failure at LC1 is obvious spallation recovery identified by the large displacement oscillations in both the scratch cycle and the residual deformation scan. Scanning probe microscopy was used to scan the region inside of the black box and the resulting image is shown on the right of the figure. The onset of lateral fracturing is seen on the left of the scanned image and this failure quickly leads to large scale spallation recovery.

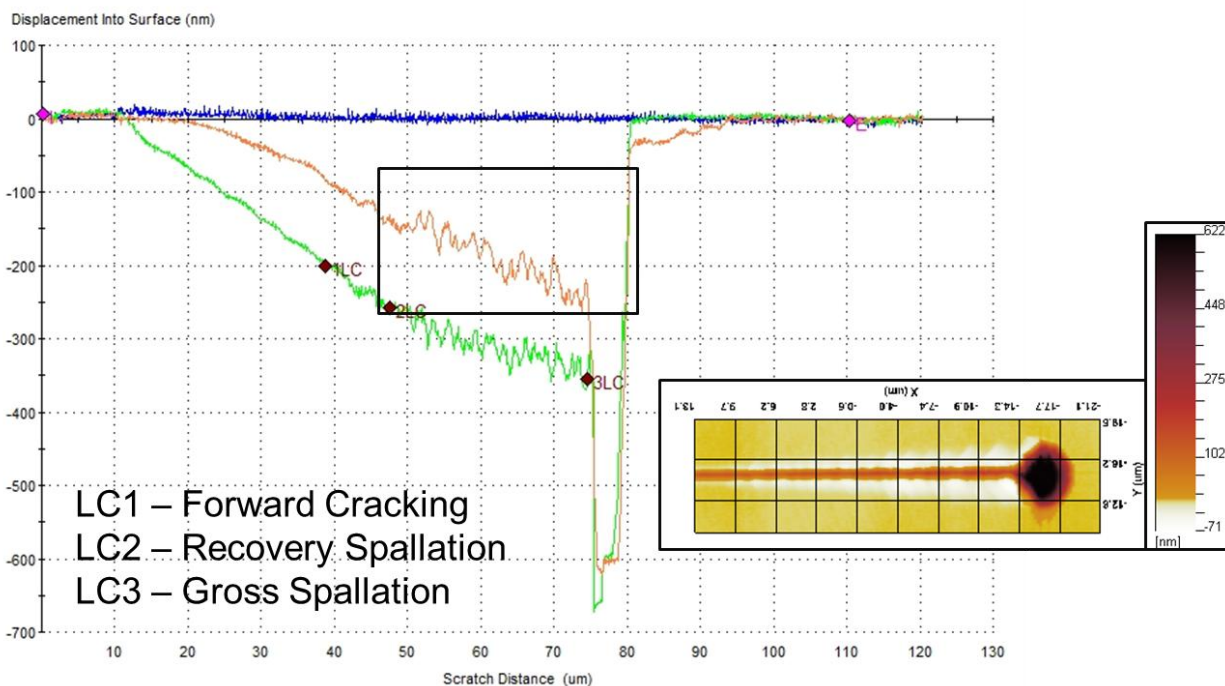


Figure 13: The figure shows typical displacement curves from the scratch tests on Wafer 10; the blue trace along the x-axis is the single-line original topography scan, the green curve is the scratch cycle, and the orange curve is the residual deformation scan. Failure in this film was different from any of the other samples tested, but it is not an uncommon failure mode in general when scratch testing low-k films. The initial failure at LC1 is cracking in the film and this is identified by a distinct slope change in the residual deformation scan suggesting that the integrity of the film was compromised at this location. Cracking is typically caused by tensile stresses behind the scratch tip and these results in forward tensile cracks in the film. A larger displacement scatter is observed shortly after LC1 as the failure mechanism switches to spallation recovery at LC2. Gross spallation occurred at LC3. The area in the black box was scanned using scanning probe microscopy and shows the entire area of failure associated with recovery spallation. It is often difficult to observe the subtle forward cracking in the scratch groove associated with the failure at LC1 and this failure is most easily identified by the 2-D scratch curves.

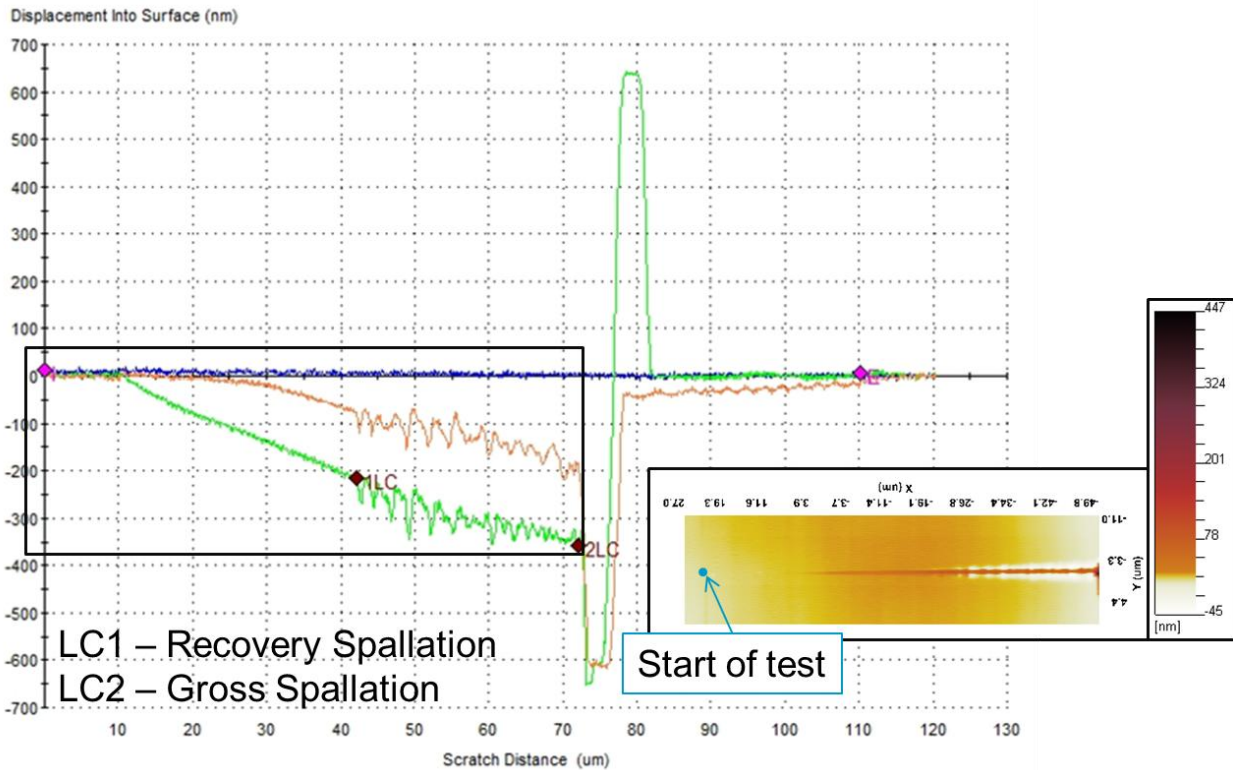


Figure 14: The figure shows typical displacement curves from the scratch tests on Wafer 13; the blue trace along the x-axis is the original topography scan, the green curve is the scratch cycle, and the orange curve is the residual deformation scan. Similar to the failure seen in Figure 9, the large displacement oscillation in the scratch curves indicate large lateral fracturing in the film and recovery spallation is occurring at LC1 for this sample. It appears that some blistering might be occurring around a scratch distance of 58 microns, but the transition in the curves is weak and, therefore, it was not identified as an independent failure mode. Gross spallation, at LC2, was the only other failure mode identified for this sample. A scan of the scratch area enclosed in the black box is provided to the right of the scratch curves. The transition from elastic deformation to plastic deformation, then on to film failure is clearly shown. The start of the scratch test on the scanned image is shown in blue and this point corresponds to the origin on the graph of the scratch curves.

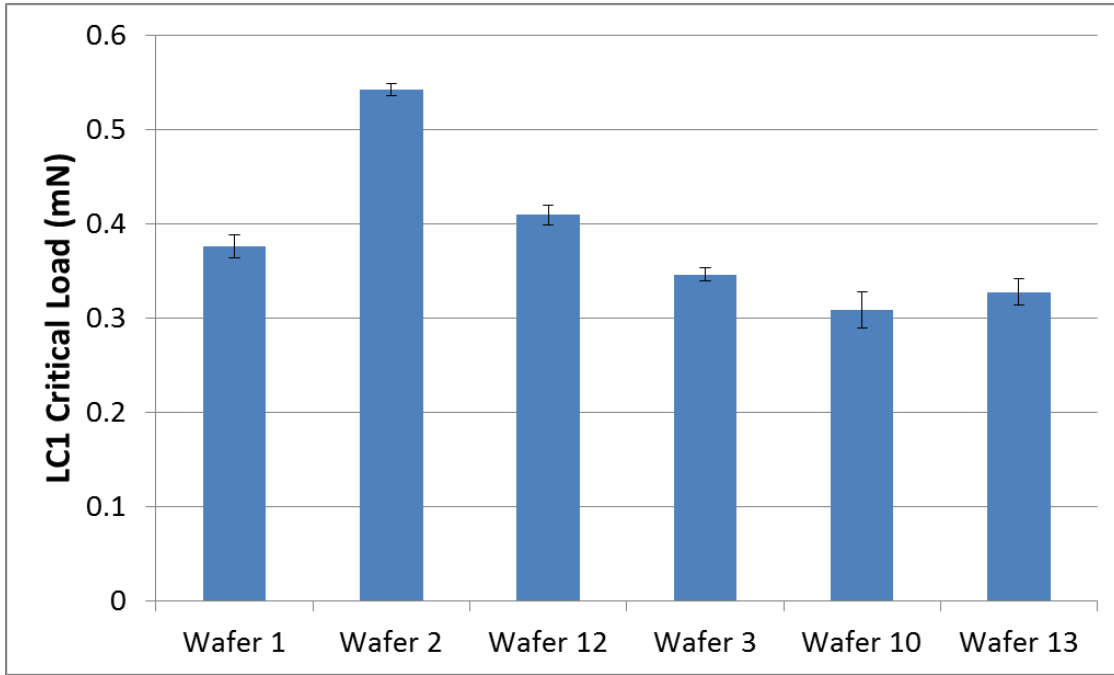


Figure 15: LC1 (initial sample failure) critical load values from Table 3 with error bars representing 1 standard deviation in the results.

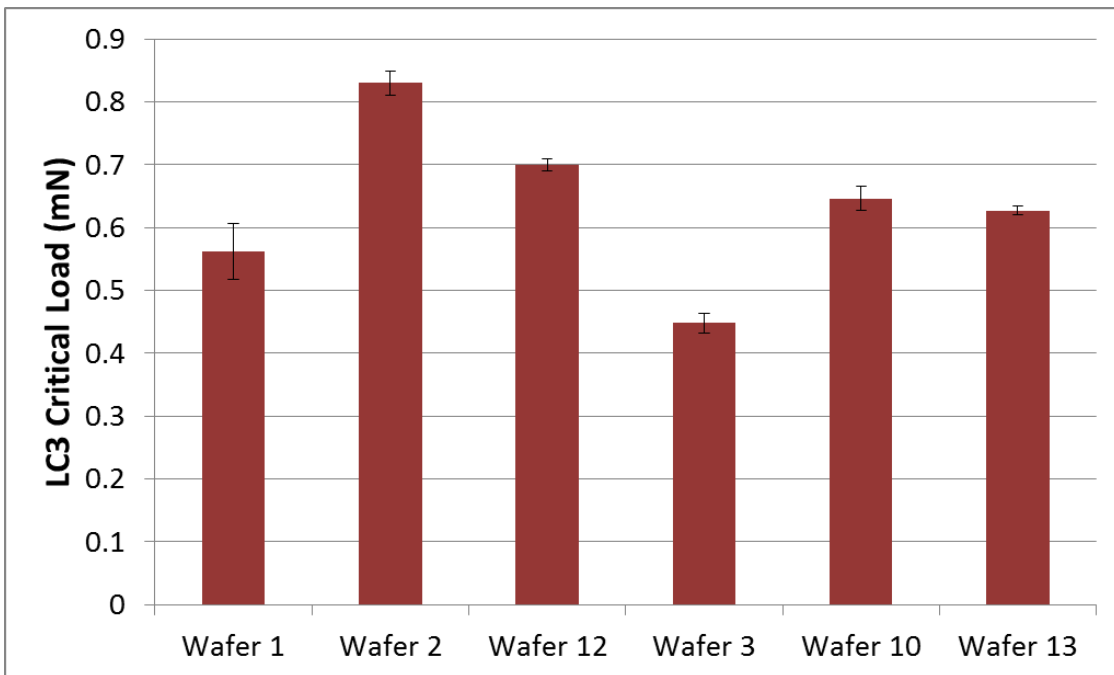


Figure 16: LC3 (gross spallation) critical load values from Table 3 with error bars representing 1 standard deviation in the results.



Analytical Services Laboratory
105 Meco Lane
Suite 100
Oak Ridge, TN 37830
(865) 978-6490 Ext. 300

ServiceLab@nanomechanicsinc.com

References

- [1] J.L. Hay and B.A. Crawford. "Measuring substrate-independent modulus of thin films." *J. Mater. Res.* **26**, 6 (2011).
- [2] W.C. Oliver and G.M. Pharr. "Measurements of hardness and elastic modulus by instrumented indentation: Advances in understanding and refinements to methodology." *J. Mater. Res.* **19**, 3 (2004).

**Please contact Bryan Crawford for more information on services offered by Nanomechanics' Analytical Services Laboratory.*